Role of deep convection in establishing the isotopic composition of water vapor in the tropical transition layer

Jamison A. Smith,[1] Andrew S. Ackerman,[2,3] Eric J. Jensen,[2] and Owen B. Toon[1,4]

Received 14 July 2005; revised 30 January 2006; accepted 2 February 2006; published 23 March 2006.

[1] The transport of H_2O and HDO within deep convection is investigated with 3-D large eddy simulations (LES) using bin microphysics. The lofting and sublimation of HDO-rich ice invalidate the Rayleigh fractionation model of isotopologue distribution within deep convection. Bootstrapping the correlation of the ratio of HDO to H_2O (δD) to water vapor mixing ratio (q_v) through a sequence of convective events produces non-Rayleigh correlations resembling observations. These results support two mechanisms for stratospheric entry. Deep convection can inject air with water vapor of stratospheric character directly into the tropical transition layer (TTL). Alternatively, moister air detraining from convection may be dehydrated via cirrus formation in the TTL to produce stratospheric water vapor. Significant production of subsaturated air in the TTL via convective dehydration is not observed in these simulations, nor is it necessary to resolve the stratospheric isotope paradox. **Citation:** Smith, J. A., A. S. Ackerman, E. J. Jensen, and O. B. Toon (2006), Role of deep convection in establishing the isotopic composition of water vapor in the tropical transition layer, *Geophys. Res. Lett.*, *33*, L06812, doi:10.1029/2005GL024078.

1. Introduction

[2] Water vapor plays an important role in the chemistry and radiation budget of the stratosphere [*Evans et al.*, 1998; *Forster and Shine*, 1999; *Tabazadeh et al.*, 2000]. An understanding of the processes that control stratospheric humidity is needed to predict changes to the ozone layer and climate.

[3] *Brewer* [1949] deduced that the primary pathway for air to enter the stratosphere from the troposphere is through the tropical tropopause because here the saturation q_v is roughly equal to the stratospheric q_v. Since then, a debate continues regarding the dominant dehydration mechanism for stratospheric air.

[4] In the gradual dehydration hypothesis, air is dehydrated by cirrus clouds formed in cold pools during slow diabatic ascent through the TTL. Here, water vapor is removed via the growth and sedimentation of ice particles [*Holton et al.*, 1995; *Jensen et al.*, 1996, 2001; *Gettelman et al.*, 2002a; *Jensen and Pfister*, 2004; *Fueglistaler et al.*, 2005]. In the convective dehydration hypothesis, air is dehydrated by the mixing of cold convective overshoots into the TTL. If ice sedimentation from these overshoots is faster than mixing with the TTL, the overshoots will dehydrate the TTL [*Sherwood and Dessler*, 2001].

[5] The isotopic composition of water vapor may serve to distinguish between dehydration mechanisms [*Moyer et al.*, 1996]. Dehydration changes δD because heavier isotopologues, like $^1H^2H^{16}O$ (HDO), have lower equilibrium vapor pressures than $^1H_2^{16}O$ (H_2O) [*van Hook*, 1968]. Therefore, δD should contain information about an air parcel's dehydration history. (In this study, δD is defined relative to Vienna Standard Mean Ocean Water, VSMOW.)

[6] Rayleigh fractionation is a pseudo-adiabatic equilibrium fractionation model [*Dansgaard*, 1964; *Jouzel and Merlivat*, 1984; *Johnson et al.*, 2001b]. Saturation is maintained via condensation, equilibrium fractionation of the isotopologues is maintained between the vapor and condensate, and the condensate is continually and completely removed via sedimentation. In this model, the HDO in the remaining vapor is depleted by preferential condensation.

[7] Lifting an air parcel from the tropical ocean surface until it has been dehydrated to a stratospheric q_v of 3.85 ppmv [*Dessler and Kim*, 1999; *Kley et al.*, 2000] via a Rayleigh process produces δD of -910‰, but observations show that δD for water vapor in the lower stratosphere is roughly -650‰ [*Moyer et al.*, 1996; *Johnson et al.*, 2001a; *Kuang et al.*, 2003; *Webster and Heymsfield*, 2003]. This underdepletion is the stratospheric isotope paradox.

[8] The modeling in this study differs from previous studies [*Moyer et al.*, 1996; *Keith*, 2000; *Johnson et al.*, 2001b; *Dessler and Sherwood*, 2003; *Gettelman and Webster*, 2005] in that the isotopic fractionation occurring within deep convection is investigated using 3-D simulations without prescribing key factors like supersaturation, sedimentation and mixing. Observations show that convection lofts condensate above the altitudes where the condensation occurs [*Smith*, 1992; *Webster and Heymsfield*, 2003]. Upon reaching subsaturated regions outside of the updrafts, this lofted condensate releases vapor with δD characteristic of condensation occurring at lower altitudes. Hence, the released water vapor is HDO-rich with respect to the Rayleigh fractionation model. After a model description, the convective redistribution of isotopologues for several simulations with varying initial δD-q_v correlations is shown and discussed.

2. Model Description

[9] The Distributed Hydrodynamic Aerosol and Radiation Modeling Application (DHARMA) is a 3-D massively

[1]Laboratory for Atmospheric and Space Physics, University of Colorado, Boulder, Colorado, USA.
[2]Earth Science Division, NASA Ames Research Center, Moffet Field, California, USA.
[3]Now at NASA Goddard Institute for Space Studies, New York, New York, USA.
[4]Also at Program in Atmospheric and Oceanic Sciences, University of Colorado, Boulder, Colorado, USA.

0094-8276/06/2005GL024078$05.00

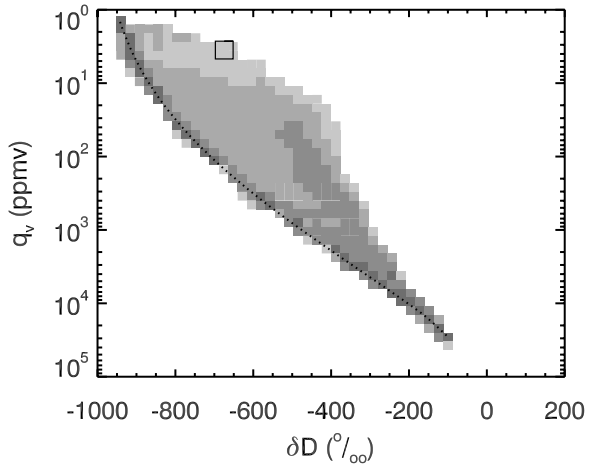

Figure 1. Probability density function of isotopic ratio of water vapor (δD) and water vapor mixing ratio (q_v) for model domain at 4 hours, excluding the nudging region. The different gray shades correspond to 1–9 (lightest), 10–99, 100–999, and 1000–9999 (darkest) grid boxes within a particular bin of δD-q_v space. The dotted line is the Rayleigh initialization. The open square represents the stratospheric entry values of δD and q_v derived from observations [*Moyer et al.*, 1996; *Johnson et al.*, 2001a].

parallel cloud model, coupling a fluid dynamics model with a cloud microphysics model. Fluid dynamics are simulated with an LES code [*Stevens and Bretherton*, 1996; *Stevens et al.*, 2002] that solves a non-hydrostatic anelastic approximation of the Navier-Stokes equation appropriate for deep convection [*Lipps and Hemler*, 1986]. Cloud microphysics are simulated for binned particle size distributions using the Community Aerosol and Radiation Model for Atmospheres (CARMA) [*Toon et al.*, 1988; *Jensen et al.*, 1994; *Ackerman et al.*, 1995; *Fridlind et al.*, 2004]. Three particle "groups" are simulated: cloud condensation nuclei (CCN), water droplets and ice crystals. The simulated microphysical processes are CCN activation, condensational growth/evaporation of cloud particles, collisional growth of cloud particles, collisional breakup of water droplets, ice nucleation and sedimentation. The microphysics affect local buoyancy and feed back on the dynamics. Open lateral boundary conditions are simulated by nudging the perimeter of the domain to the initial conditions. The auxiliary material contains additional model description.[1]

3. Model Results and Discussion

[10] The isotopologue distribution within deep convection is shown for varying initial δD-q_v correlations. A Rayleigh δD-q_v correlation is used for the first simulation. The anvil's horizontal extent is greatest at 13 km with overshooting turrets reaching 17 km. The δD-q_v probability density function (PDF) at 4 hours is shown in Figure 1. The convection has produced a highly disperse PDF consistent with in situ measurements [*Webster and Heymsfield*, 2003]. This variability results from the mixing of the non-Rayleigh convected air with the Rayleigh initialization.

[11] Three additional simulations with different initial δD-q_v correlations are also shown. After cloud dissipation (through precipitation and evaporation) ~14 hours into the first simulation, the average correlation from the convectively perturbed region ($9 \times 9 \times 17$ km^3) is used for the next initialization. This bootstrapping is repeated twice more for a total of four simulations. Figure 2 shows the final correlations for the convectively perturbed region of all four simulations. The first convective event strongly perturbs the initially Rayleigh atmosphere, but subsequent events produce smaller perturbations. The final PDF of the fourth simulation is also shown. There is less variability in this distribution since the detraining vapor is similar to the initial vapor set by the previous simulation.

[12] Admittedly, the convective correlations have not converged after this bootstrapping sequence, but it is shown below that these correlations do resemble the tropical observations, probably because other transport and cloud processes counter the influence of deep convection on water vapor in the tropics. Estimates from satellite observations of the tropics show that the direct influence of convection on the TTL is not overwhelming, with convective turnover times (τ) comparable with the time scales for meridional transport and diabatic ascent ($\tau \sim 1$ month at 12.5 km and ~1 year at 16 km [*Gettelman et al.*, 2002b]). Additional discussion of simulation convergence appears in the auxiliary material.

[13] Figure 3 shows that the convective correlations resemble remote sensing observations [*Kuang et al.*, 2003]. A discrepancy does exist between the shapes of the observed and simulated correlations. This discrepancy

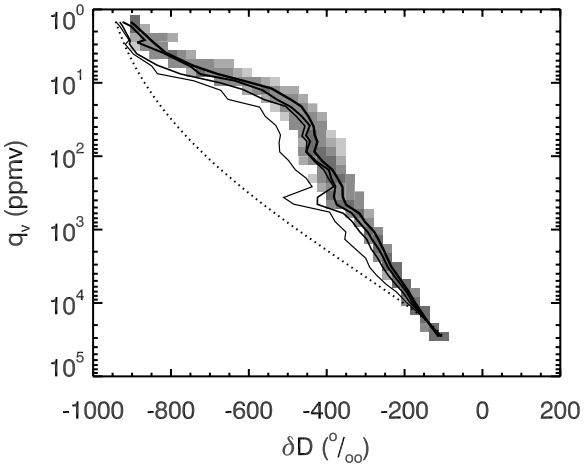

Figure 2. Final average correlations within the convectively perturbed subdomain ($9 \times 9 \times 17$ km^3) for each simulation (solid lines). Increasing line thickness indicates increasing simulation number. The dotted line is the Rayleigh correlation. Also shown is the probability density function of the isotopic ratio of water vapor (δD) and the water vapor mixing ratio (q_v) for the model domain below 17 km, excluding the nudging region, after cloud dissipation for the fourth simulation. The gray scale is identical to Figure 1.

[1]Auxiliary material is available at ftp://ftp.agu.org/apend/gl/2005gl024078.

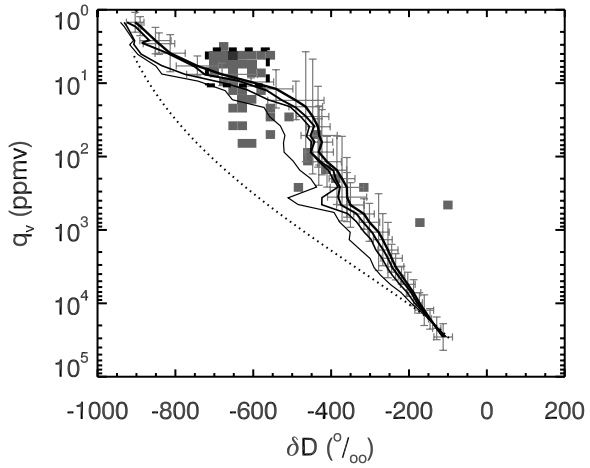

Figure 3. Probability density function of the isotopic ratio of water vapor (δD) and the water vapor mixing ratio (q_v) for remote sensing observations of the tropics below 19 km [*Kuang et al.*, 2003]. Light and dark gray correspond to 1–9 and 10–99 observations respectively within a particular bin of δD-q_v space. The dashed box represents the remote sensing observations of the TTL. The box is centered on the mean of δD and ln q_v, and it encompasses the 2σ variability. The black lines are identical to Figure 2. The error bars represent the 2σ variability within the domain below 17 km for the fourth simulation.

arises from the fact that the observed air has been processed by a variety of convective events with varying intensities. Future simulations of an ensemble of events should improve the agreement between the observed and simulated shapes.

[14] For air dehydrated to 3.85 ppmv in the simulations, δD is between −856 and −736‰, as shown in Figure 4. These δD are richer than the observed Rayleigh fractionation value (−910‰) but poorer than the stratospheric entry values (−670 and −679‰) [*Moyer et al.*, 1996; *Johnson et al.*, 2001a]. Improving ice physics in the model may improve the agreement with observations, which might account for the simulated ice being slightly HDO-poor as well. For observations of upper tropospheric air containing more than 80% of total water as ice, δD_{ice} is −130 ± 83‰ (1σ) [*Webster and Heymsfield*, 2003], and for simulated air above 13 km with the same ice fraction, δD_{ice} is −320 ± 20‰ (1σ). Excessive precipitation in the model could be responsible for this discrepancy. The discrepancy might also result from neglecting the spatial inhomogeneity of δD within each ice particle, i.e., the HDO-rich interior may be leaking out prematurely during sublimation. The internal structure of δD within cloud ice will be examined in a future study, but this internal inhomogeneity may not be significant if vertical eddies repeatedly deposit and strip off the outermost molecular layers of the cloud particles, thereby partially homogenizing the internal isotopologue distribution. Other model uncertainties include the sensitivity to meteorology, aerosol abundance and shortcomings in the microphysics model such as the treatment of ice collisions.

[15] Similar to previous studies [*Moyer et al.*, 1996; *Keith*, 2000; *Kuang et al.*, 2003], Figure 4 shows the δD-q_v correlations for air parcels detraining from convection and undergoing Rayleigh fractionation during gradual dehydration. With equilibrium fractionation occurring from altitudes of 13, 14 and 15 km, δD is −804, −746 and −711‰ respectively when q_v reaches 3.85 ppmv. These δD are poorer in HDO than stratospheric water vapor, but if the kinetic isotope effect [*Jouzel and Merlivat*, 1984] is included with a fixed supersaturation of 0.6, δD is −680, −644 and −632‰ respectively. As noted by *Gettelman and Webster* [2005], the high supersaturations associated with ice nucleation improve the agreement between the slow ascent hypothesis and observations.

[16] An argument for the convective dehydration mechanism comes from remote sensing observations showing that δD does not decrease with respect to either altitude or q_v in the TTL as shown in Figure 3 [*Kuang et al.*, 2003]. Gradual dehydration must be accompanied by a decreasing δD, so a lack of decrease in δD could invalidate the gradual dehydration mechanism [*Dessler and Sherwood*, 2003; *Kuang et al.*, 2003]. The fields of q_v and δD, however, are variable on scales smaller than the vertical resolution of the remote sensing observations, and a non-decreasing δD may be produced by averaging two fields with a nonlinear relationship over the sample volume [*Webster and Heymsfield*, 2003]. In addition, individual profiles of δD show structure that is absent in the average profile, and this structure can be traced to the origin of the air whether tropospheric or stratospheric [*Gettelman and Webster*, 2005].

[17] Overshooting convection occurs in these simulations, but convective dehydration does not occur because the lofted ice does not sediment before the overshoots mix with the environment. Admittedly, more simulations should

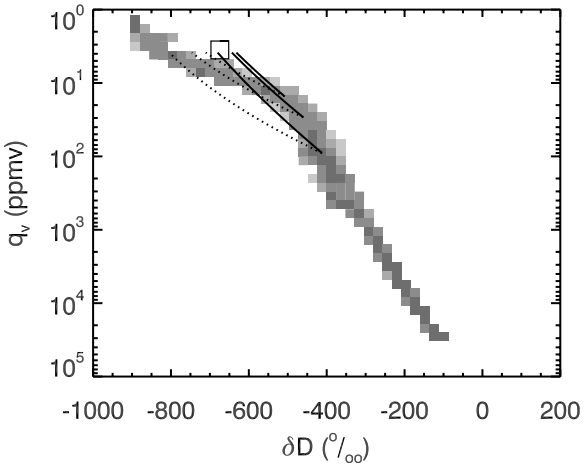

Figure 4. Probability density function of the isotopic ratio of water vapor (δD) and water vapor mixing ratio (q_v) for the model domain below 17 km, excluding the nudging region, after cloud dissipation for the fourth simulation. The gray scale is identical to Figure 1. The dotted lines represent equilibrium Rayleigh fractionation occurring during gradual dehydration for air parcels detraining from convection at 13, 14 and 15 km. The solid lines account for the kinetic isotope effect on Rayleigh fractionation occurring at a supersaturation of 0.6. The open square represents observed stratospheric entry values of δD and q_v [*Moyer et al.*, 1996; *Johnson et al.*, 2001a].

be performed with a variety of soundings and sources to generalize this result, but in the simulations presented here, convection consistently tends to drive the atmosphere toward saturation via sublimation of small ice particles (see auxiliary material for further discussion of convective dehydration).

4. Conclusions

[18] The simulated field of δD within deep convection is enriched relative to Rayleigh fractionation due to the lofting of HDO-rich cloud ice from lower altitudes to higher altitudes where the ice sublimes. Convective air with stratospheric q_v is slightly HDO-poor, but this discrepancy can probably be attributed to small model biases. Convective dehydration is insignificant in these simulations. The simulated convection does directly inject air with stratospheric values of δD and q_v into the TTL, but without convective dehydration. A second dehydration mechanism consistent with our simulations involves the detrainment of moister air into the TTL followed by gradual dehydration in cirrus clouds. The large supersaturation needed for ice nucleation improves the agreement between the gradual dehydration mechanism and observations.

[19] **Acknowledgments.** This work was supported by NASA grants NAG5-11474 and NNG04GK37G. Computing resources were provided by the Department of Energy (DOE) National Energy Research Scientific Computing Center (NERSC). We thank Zhiming Kuang for kindly providing remote sensing data.

References

Ackerman, A. S., O. B. Toon, and P. V. Hobbs (1995), A model for particle microphysics, turbulent mixing, and radiative transfer in the stratocumulus-topped marine boundary layer and comparisons with measurements, *J. Atmos. Sci.*, *52*, 1204–1236.

Brewer, A. W. (1949), Evidence for a world circulation provided by the measurements of helium and water vapour distribution in the stratosphere, *Q. J. R. Meteorol. Soc.*, *75*, 351–363.

Dansgaard, W. (1964), Stable isotopes in precipitation, *Tellus*, *16*, 436–468.

Dessler, A. E., and H. Kim (1999), Determination of the amount of water vapor entering the stratosphere based on HALOE data, *J. Geophys. Res.*, *104*, 30,605–30,607.

Dessler, A. E., and S. C. Sherwood (2003), A model of HDO in the tropical tropopause layer, *Atmos. Chem. Phys.*, *3*, 2173–2181.

Evans, S. J., R. Toumi, J. E. Harries, M. P. Chipperfield, and J. M. Russell (1998), Trends in stratospheric humidity and the sensitivity of ozone to these trends, *J. Geophys. Res.*, *103*, 8715–8725.

Forster, P. M. F., and K. P. Shine (1999), Stratospheric water vapor changes as a possible contributor to observed stratospheric cooling, *Geophys. Res. Lett.*, *26*, 3309–3312.

Fridlind, A. M., et al. (2004), Evidence for the predominance of mid-tropospheric aerosols as subtropical anvil cloud nuclei, *Science*, *304*, 718–722.

Fueglistaler, S., M. Bonazzola, P. H. Haynes, and T. Peter (2005), Stratospheric water vapor predicted from the Lagrangian temperature history of air entering the stratosphere in the tropics, *J. Geophys. Res.*, *110*, D08107, doi:10.1029/2004JD005516.

Gettelman, A., and C. R. Webster (2005), Simulations of water isotope abundances in the upper troposphere and lower stratosphere and implications for stratosphere troposphere exchange, *J. Geophys. Res.*, *110*, D17301, doi:10.1029/2004JD004812.

Gettelman, A., W. J. Randel, F. Wu, and S. T. Massie (2002a), Transport of water vapor in the tropical tropopause layer, *Geophys. Res. Lett.*, *29*(1), 1009, doi:10.1029/2001GL013818.

Gettelman, A., M. L. Salby, and F. Sassi (2002b), Distribution and influence of convection in the tropical tropopause region, *J. Geophys. Res.*, *107*(D10), 4080, doi:10.1029/2001JD001048.

Holton, J. R., P. H. Haynes, M. E. McIntyre, A. R. Douglas, R. B. Rood, and L. Pfister (1995), Stratosphere-troposphere exchange, *Rev. Geophys.*, *33*, 403–440.

Jensen, E., and L. Pfister (2004), Transport and freeze-drying in the tropical tropopause layer, *J. Geophys. Res.*, *109*, D02207, doi:10.1029/2003JD004022.

Jensen, E. J., O. B. Toon, D. L. Westphal, S. Kinne, and A. J. Heymsfield (1994), Microphysical modeling of cirrus: 1. Comparison with 1986 FIRE IFO measurements, *J. Geophys. Res.*, *99*, 10,421–10,442.

Jensen, E. J., O. B. Toon, L. Pfister, and H. B. Selkirk (1996), Dehydration of the upper troposphere and lower stratosphere by subvisible cirrus clouds near the tropical tropopause, *Geophys. Res. Lett.*, *23*, 825–828.

Jensen, E. J., L. Pfister, A. S. Ackerman, A. Tabazadeh, and O. B. Toon (2001), A conceptual model of the dehydration of air due to freeze-drying by optically thin, laminar cirrus rising slowly across the tropical tropopause, *J. Geophys. Res.*, *106*, 17,237–17,252.

Johnson, D. G., K. W. Jucks, W. A. Traub, and K. V. Chance (2001a), Isotopic composition of stratospheric water vapor: Measurements and photochemistry, *J. Geophys. Res.*, *106*, 12,211–12,217.

Johnson, D. G., K. W. Jucks, W. A. Traub, and K. V. Chance (2001b), Isotopic composition of stratospheric water vapor: Implications for transport, *J. Geophys. Res.*, *106*, 12,219–12,226.

Jouzel, J., and L. Merlivat (1984), Deuterium and oxygen 18 in precipitation: Modeling of the isotopic effects during snow formation, *J. Geophys. Res.*, *89*, 11,749–11,757.

Keith, D. W. (2000), Stratosphere-troposphere exchange: Inferences from the isotopic composition of water vapor, *J. Geophys. Res.*, *105*, 15,167–15,173.

Kley, D., J. M. Russell, and C. Phillips (Eds.) (2000), SPARC assessment of upper tropospheric and stratospheric water vapour, *WCRP Rep. 113/SPARC Rep. 2*, World Clim. Res. Program, Paris.

Kuang, Z., G. C. Toon, P. O. Wennberg, and Y. L. Yung (2003), Measured HDO/H_2O ratios across the tropical tropopause, *Geophys. Res. Lett.*, *30*(7), 1372, doi:10.1029/2003GL017023.

Lipps, F. B., and R. S. Hemler (1986), Numerical simulation of deep tropical convection associated with large-scale convergence, *J. Atmos. Sci.*, *43*, 1796–1816.

Moyer, E. J., F. W. Irion, Y. L. Yung, and M. R. Gunson (1996), ATMOS stratospheric deuterated water and implications for troposphere-stratosphere transport, *Geophys. Res. Lett.*, *23*, 2385–2388.

Sherwood, S. C., and A. E. Dessler (2001), A model for transport across the tropical tropopause, *J. Atmos. Sci.*, *58*, 765–779.

Smith, R. B. (1992), Deuterium in North Atlantic storm tops, *J. Atmos. Sci.*, *49*, 2041–2057.

Stevens, D. E., and S. Bretherton (1996), A forward-in-time advection scheme and adaptive multilevel flow solver for nearly incompressible flow, *J. Comput. Phys.*, *129*, 284–295.

Stevens, D. E., A. S. Ackerman, and C. S. Bretherton (2002), Effects of domain size and numerical resolution on the simulation of shallow cumulus convection, *J. Atmos. Sci.*, *59*, 3285–3301.

Tabazadeh, A., M. L. Santee, M. Y. Danilin, H. C. Pumphrey, P. A. Newman, P. J. Hamill, and J. L. Mergenthaler (2000), Quantifying denitrification and its effect on ozone recovery, *Science*, *288*, 1407–1411.

Toon, O. B., R. P. Turco, D. Westphal, R. Malone, and M. S. Liu (1988), A multidimensional model for aerosols: Description of computational analogs, *J. Atmos. Sci.*, *45*, 2123–2143.

van Hook, W. A. (1968), Vapor pressures of the isotopic waters and ices, *J. Phys. Chem.*, *72*, 1234–1244.

Webster, C. R., and A. J. Heymsfield (2003), Water isotope ratios D/H, $^{18}O/^{16}O$, $^{17}O/^{16}O$ in and out of clouds map dehydration pathways, *Science*, *302*, 1743–1745.

A. S. Ackerman, NASA Goddard Institute for Space Studies, 2880 Broadway, New York, NY 10025, USA.

E. J. Jensen, Earth Science Division, NASA Ames Research Center, Mail Stop 245-4, Moffet Field, CA 94035, USA.

J. A. Smith and O. B. Toon, Laboratory for Atmospheric and Space Physics, University of Colorado, Boulder, CO 80309, USA. (jamisons@lasp.colorado.edu)